EUKARYOTIC CELL, Jan. 2010, p. 215–223 Vol. 9, No. 1
1535-9778/10/$12.00 doi:10.1128/EC.00214-09

Identification and Partial Characterization of a Dynamin-Like Protein, EhDLP1, from the Protist Parasite *Entamoeba histolytica*▽†

Ruchi Jain,[1]‡ Shiteshu Shrimal,[1] Sudha Bhattacharya,[2] and Alok Bhattacharya[1]*

School of Life Sciences, Jawaharlal Nehru University, New Mehrauli Road, New Delhi, India,[1] and School of Environmental Sciences, Jawaharlal Nehru University, New Mehrauli Road, New Delhi, India[2]

Received 23 July 2009/Accepted 2 November 2009

The dynamin superfamily of proteins includes a large repertoire of evolutionarily conserved GTPases that interact with different subcellular organelle membranes in eukaryotes. Dynamins are thought to participate in a number of cellular processes involving membrane remodeling and scission. Dynamin-like proteins (DLPs) form a subfamily of this vast class and play important roles in cellular processes, such as mitochondrial fission, cytokinesis, and endocytosis. In the present study, a gene encoding a dynamin-like protein (EhDLP1) from the protist parasite *Entamoeba histolytica* was identified and the protein was partially characterized using a combination of *in silico*, biochemical, and imaging methods. The protein was capable of GTP binding and hydrolysis, lipid binding, and oligomerization. Immunofluorescence studies showed the protein to be associated with the nuclear membrane. A mutant of EhDLP1 lacking GTP binding and hydrolyzing activities did not associate with the nuclear membrane. The results suggest a nucleus-associated function for EhDLP1.

Dynamins are a vast family of GTPases implicated in myriad processes, some of which lead to alteration of membrane structure (22). Classical dynamins, such as mammalian dynamins 1 to 3 (5) and the *shibire* protein from *Drosophila melanogaster* (29), are required mainly for scission of vesicles, acting as mechanoenzymes or molecular switches (12). In addition, several dynamin-like proteins (DLPs) have been identified in different organisms ranging from yeast to mammals. DLPs play a key role in the division of organelles such as chloroplasts, mitochondria, and peroxisomes (15, 22). For example, *Candida albicans* Vps1 has been shown to be associated with virulence-related phenotypes like filamentation and biofilm formation (2). DLPs have also been identified in protists. Downregulation or ablation of the gene products in protists by RNA interference or other methods has helped to decipher the multiple functions carried out by these proteins. These include mitochondrial division and endocytosis in *Trypanosoma brucei* (6, 20), cytokinesis in *Dictyostelium discoideum* (31), phagocytosis in *Paramecium* species (30), endocytic transport in *Giardia lamblia* (11), and biogenesis of secretory vesicles in *Toxoplasma gondii* (4). Apart from cellular membranes, some DLPs may also associate with nuclear membranes. Recently, a study on *Tetrahymena thermophila* reported the requirement of Drp6 for macronuclear development (23). The human DLP MxB has been shown previously to localize to the cytoplasmic face of the nuclear envelope and is involved in regulation of nuclear import (14). Dynamins and DLPs share a minimal domain architecture which includes an N-terminal GTPase domain, a middle domain, and a GTPase effector domain (GED). The GED is involved in enzyme oligomerization and the regulation of the GTPase activity. The GTPase domain contains a well-conserved GTP binding motif required for guanine-nucleotide binding and hydrolysis (22). DLPs lack a pleckstrin homology (PH) domain and a proline-rich domain (PRD), normally associated with protein-lipid and protein-protein interaction.

The endocytic, secretory, and adhesion pathways of the parasite *Entamoeba histolytica* play crucial roles in nutrient uptake, host cell destruction, and the endocytosis of gut resident bacteria, erythrocytes, and cell debris (21). The trophozoites of *E. histolytica* are known to have robust endocytic capabilities, turning over approximately a third of their cellular volume every hour (1, 19). The presence of a classical receptor-mediated pathway has not yet been clearly demonstrated, though some of the molecules involved in this pathway, such as clathrin, have been identified in *E. histolytica* (28). Typical eukaryotic cytoplasmic organelles have not been observed in this organism. However, the functional equivalents of a Golgi network and an endoplasmic reticulum are reported to be present (3, 26). *Entamoeba* also contains a genomeless variant of mitochondria, termed mitosomes (17). The division or biogenesis of these organelles during cell division is not understood. Nuclear division in *E. histolytica* occurs without nuclear membrane dissolution and reassembly. Since dynamins and DLPs are known to be involved in endocytosis and organelle division, it is likely that these proteins may be performing similar functions in this organism. Although the *E. histolytica* genome encodes putative dynamins and DLPs, none of these have been characterized. In order to understand the roles of these molecules in amebic biology, we have initiated studies to characterize these proteins from *E. histolytica*. Here, we report the basic characterization of *E. histolytica* dynamin-like protein 1 (EhDLP1).

MATERIALS AND METHODS

Strains and growth conditions. *E. histolytica* strain HM1:IMSS clone 6 was maintained and grown in TYI-S-33 medium (10a) containing 125 μl of 250 U ml^{-1}

* Corresponding author. Mailing address: Lab 118, School of Life Sciences, Jawaharlal Nehru University, New Mehrauli Road, New Delhi, India 110067. Phone: 91-11-26704516. Fax: 91-11-26745816. E-mail: alok0200@mail.jnu.ac.in.

† Supplemental material for this article may be found at http://ec.asm.org/.

‡ Present address: Department of Internal Medicine, Infectious Diseases, Yale University School of Medicine, New Haven, CT 06510.

▽ Published ahead of print on 13 November 2009.

benzyl penicillin and 0.25 mg ml^{-1} streptomycin per 100 ml of medium. Neomycin (Sigma) was added at 10 μg ml^{-1} for maintaining transgenic cell lines.

Escherichia coli strains (BL21 and DH5α) were maintained in Luria broth containing 100 μg ml^{-1} ampicillin or 30 μg ml^{-1} kanamycin as indicated.

Isolation of EhDLP1 gene and cloning into different vectors. All the sequences analyzed were retrieved from the *E. histolytica* genome databases at The Institute for Genomic Research (TIGR; http://www.tigr.org/tdb/e2k1/eha1) and Pathema (http://pathema.jcvi.org/cgi-bin/Entamoeba/PathemaHomePage.cgi). The identified genes from *E. histolytica* genome databases were then further analyzed and verified by a BLAST.CD search of the NCBI database (http://www.ncbi.nlm.nih.gov/BLAST), and Pfam (http://www.pfam.sanger.ac.uk/search) was used to identify the domains in EhDLP1.

The EhDLP1 gene was amplified from *E. histolytica* HM1:IMSS genomic DNA by PCR using the following primers: forward, 5′ GACTATGAAAAGTC TTATTCCAGTT 3′, and reverse, 5′ GACGTTAATTAACTTTGATTGTAAC 3′. The amplicon (2,047 bp) was cloned into the pGEM-T Easy vector (Promega) and subcloned into the NcoI/SalI sites of the pET-30(a) vector (Novagen). BL21(DE3) cells were transformed with the resulting construct and used for the production of recombinant EhDLP1 (rEhDLP1) protein.

The EhDLP1 gene was also cloned upstream of the green fluorescent protein (GFP) gene in the pEh-NEO-GFP vector (13). The primers used were as follows: forward, 5′ CCCGGTACCATGAAAAGTCTTATTCCA 3′, and reverse, 5′ GG GGGTACCTTAATTAACTTTGATTGT 3′.

In order to generate the lysine mutant of EhDLP1 protein, site-directed mutagenesis was carried out according to the instructions of the mutagenesis kit manufacturer (Stratagene). The primers used for mutagenesis were as follows: forward, 5′ GGGTCTCAAAGTGCTGGTGCATCATCTGTATTAGAAAG 3′, and reverse, 5′ CTTTCTAATACAGATGATGCACCAGCACTTTGAGACCC 3′.

All constructs were verified by nucleotide sequencing.

Expression and purification of rEhDLP1 from *E. coli*. *E. coli* strain BL21(DE3) was transformed with the constructs expressing EhDLP1 or the K38A mutant of EhDLP1 (hereinafter referred to as EhDLP1-K38A) in order to produce the recombinant proteins by inducing the cultures with IPTG (isopropyl-β-D-thiogalactopyranoside; 0.1 mM for EhDLP1 and 0.4 mM for EhDLP1-K38A) for 3 h at 37°C with aeration.

The expressed proteins were purified using Ni^{2+}-nitrilotriacetic acid (NTA) affinity chromatography, as the recombinant proteins were each carrying a His tag at the amino terminus. Briefly, the induced bacterial cells were harvested at 6,000 rpm for 5 min at 4°C. The cells were lysed by incubation of the pellet in lysis buffer (1× phosphate-buffered saline [PBS] in 20 mM imidazole) containing 200 μg/ml lysozyme, 1 mM dithiothreitol (DTT), and a protease inhibitor cocktail, followed by sonication. The recombinant proteins were further recovered from the pellets by solubilization in 0.2% Sarkosyl solution (0.2% *N*-lauryl sarcosine solution containing 25 mM triethanolamine, 20 mM imidazole, and 1 mM EDTA [pH 8.0], supplemented with 0.1% 0.1 M $CaCl_2$ and Triton X-100) for 1 h at 4°C. The supernatant containing the desired protein was loaded onto Ni^{2+}-NTA beads, and the proteins were purified per the instructions of the bead manufacturer (Amersham). The fractions were analyzed by SDS–10% PAGE. Fractions containing purified fusion protein were pooled and dialyzed against HCB 300 (20 mM HEPES [pH 7.2], 2 mM EGTA, 2 mM $MgCl_2$, 1 mM DTT, and 300 mM NaCl) containing 10% glycerol. The protein samples obtained were further concentrated with an Amicon concentrator (with a cutoff at a molecular weight of 30,000) and stored as small aliquots at −80°C.

EhDLP1 antisera. The purified antigen (EhDLP1, as described above) was dialyzed against PBS. Rabbits were immunized subcutaneously four times at multiple sites with 100 μg of protein per injection and an interval of 3 weeks between each injection. The first dose of the protein was emulsified with complete Freund's adjuvant, while incomplete Freund's adjuvant was used for the subsequent booster immunization. Sera from immunized rabbits were collected 2 weeks after the last booster and stored in aliquots at −80°C.

Subcellular localization of EhDLP1 in *Entamoeba* lysate. To separate the nuclear fraction from the cytoplasm and the membrane fraction, the protocol described by Dey et al. (10) was followed. Briefly, 10^7 cells growing in log phase were harvested at 280 × *g* for 7 min at 4°C and resuspended in 2 ml lysis buffer (10 mM HEPES [pH 7.5], 1.5 mM $MgCl_2$, 10 mM KCl, 0.5 mM DTT, 0.2% Nonidet P-40 detergent, and protease inhibitors). The suspension was incubated on ice for 15 min and then centrifuged at 3,000 × *g* for 10 min at 4°C. The pellet thus obtained contained the nuclear fraction, and the supernatant was ultracentrifuged at 100,000 × *g* for 30 min at 4°C to obtain the cytoplasmic and membrane fractions. The nuclear pellet was resuspended in 50 μl of the lysis buffer, and the protein content of each fraction was estimated by the bicinchoninic acid assay.

GTP binding and hydrolysis assays. GTP binding assays were performed in two separate ways: (i) covalent cross-linking of [α-^{32}P]GTP to the purified rEhDLP1 or mutant protein under UV light exposure and (ii) use of a filter binding assay. To perform the UV cross-linking assay, a 2-μg sample of purified rEhDLP1 or mutant protein in buffer containing 20 mM HEPES (pH 7.2), 2 mM $MgCl_2$, 1 mM DTT, 10 μCi [α-^{32}P]GTP, 150 mM NaCl, and 10% glycerol was incubated on ice for 10 min and then exposed to UV light irradiation (wavelength, 254 nm) at a distance of 5 cm for 30 min at 4°C with a system from Stratagene. After termination of UV exposure, 0.8 μl of 100 mM dGTP and 20 μg of bovine serum albumin (BSA) were added to the reaction mixtures. Proteins were precipitated by incubation in 10% trichloroacetic acid for 45 min at 4°C and washed with acetone. These proteins were separated by SDS-PAGE, and the labeled proteins were visualized by using a PhosphorImager.

Alternatively, rEhDLP1 or the mutant (2 μg) was incubated in buffer containing 20 mM HEPES (pH 7.2), 2 mM $MgCl_2$, 1 mM DTT, 150 mM NaCl, and 1 μCi [α-^{32}P]GTP for 20 min at 4°C. The samples were loaded onto a nitrocellulose membrane (0.45-μm pore size) in a filter dot blot apparatus under a vacuum. The filter was rapidly washed once with 250 μl of cold buffer. The dried filter was imaged using a PhosphorImager, and spots were quantified using MultiImage software.

GTP hydrolysis by rEhDLP1 or the mutant was monitored as the hydrolysis of [γ-^{32}P]GTP by the purified proteins. One microgram of purified protein was incubated in 1× GTPase buffer (20 mM HEPES [pH 7.4], 2 mM $MgCl_2$, 150 mM NaCl, 1 mM DTT) containing 1.0 μCi of [γ-^{32}P]GTP in a 20-μl reaction volume for 15 min at room temperature. The reaction was terminated by the addition of 1× SDS sample buffer, and the reactants were resolved by polyethyleneimine thin-layer chromatography (TLC) using 0.75 M KH_2PO_4 (pH 3.75) as the solvent phase. The TLC plates were then exposed to a PhosphorImager or an X-ray film.

Velocity sedimentation assay. Three to five micrograms of purified protein dialyzed against high-salt-concentration buffer HCB 300 was used for each 100-μl total reaction volume. The final salt concentration was then varied to either 150 or 50 mM NaCl by using HCB 0, which contains 0 mM NaCl. Three to five micrograms of rEhDLP1 or the mutant protein was added to buffers with different salt concentrations in the ultracentrifuge tubes. These tubes were then incubated for 10 min at room temperature and centrifuged at 100,000 × *g* for 10 min. The supernatants containing unassembled proteins were then carefully collected and analyzed by SDS-PAGE after precipitation with trichloroacetic acid. The pellet containing the assembled protein oligomers was also resuspended in SDS-PAGE sample buffer and analyzed by SDS-PAGE.

Lipid binding assay. Membrane binding of rEhDLP1 was checked by monitoring the ability of the protein to make tubes upon incubation with phosphatidylcholine (PC) liposomes. To prepare PC liposomes, synthetic PC (Avanti Polar Lipids) was resuspended at a concentration of 3 mg/ml in chloroform and then dried using nitrogen gas with constant swirling. The dried lipids form a thin layer on the surface of the glass tube. These dried lipids were then resuspended in HCB 100 (20 mM HEPES [pH 7.2], 2 mM $MgCl_2$, 2 mM EGTA, 1 mM DTT, and 100 mM NaCl) to a final concentration of 3 mg/ml. The glass tube containing the lipid suspension was subjected to a vortex in a water sonicator five to six times until the solution became turbid.

Protein-lipid tubes were monitored by incubating the target protein (rEhDLP1) with PC liposomes in a ratio of 1:1 with 0.1- to 0.25-mg/ml concentrations of both protein and lipid for 3 to 4 h at room temperature. In one of the reactions, the tubes were incubated with 1 mM GTP for 30 min at 37°C prior to the preparation of a sample for electron microscopy.

All the samples prepared as described above (liposomes alone, lipid tubes, and the lipid tubes incubated with GTP) were examined by transmission electron microscopy at the All India Institute of Medical Science (New Delhi). Samples were diluted to 0.1 mg/ml, adsorbed to 400-mesh carbon-coated electron microscopy grids, and negatively stained with 2% uranyl acetate before being air dried. Electron micrographs were obtained using a Philips 400 or CM120 electron microscope at 100 kV and recorded at a defocus level of 1.15 mm.

Immunofluorescence assays. *E. histolytica* resuspended in warm incomplete TYI-33 medium (TYI-S-33 without serum) was transferred onto prewarmed, acetone-cleaned coverslips in a petri dish and allowed to adhere for 10 min at 37°C. The culture medium was removed, and coverslips were fixed with 3.7% prewarmed paraformaldehyde (PFA) for 30 min. After fixation, the cells were permeabilized with 1% Triton–PBS for 1 min. The cells were then washed with PBS and quenched for 30 min in PBS containing 50 mM NH_4Cl. The coverslips were blocked with 1% BSA–PBS for 30 min and then incubated with primary antibody at 37°C for 1 h. These coverslips were then washed with PBS followed by 1% BSA–PBS before being incubated with secondary antibody for 30 min at 37°C. The following antibody dilutions were used: anti-EhDLP1, 1:50; anti-GFP, 1:200; and anti-rabbit Alexa 488, 1:200. To stain DNA, DNA-specific dye

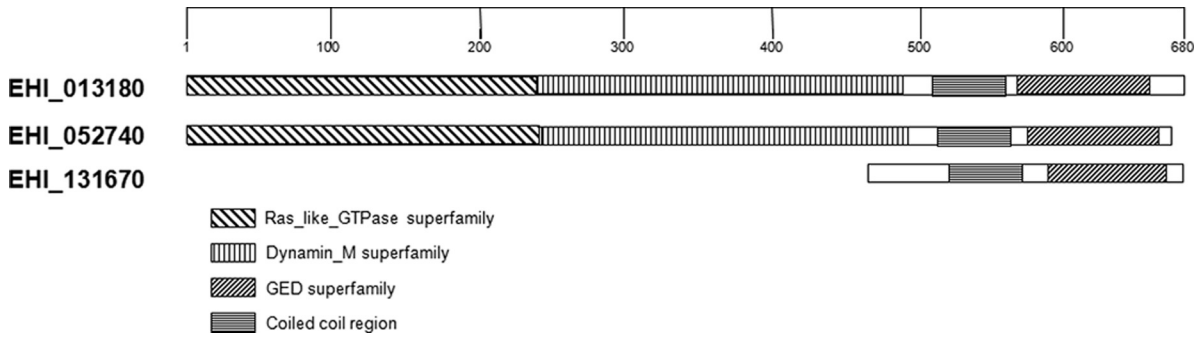

FIG. 1. Primary sequence analysis of EhDLP1. Shown is a schematic representation of the products encoded by the three genes present in the Pathema database, annotated as DLPs with domain assignments and secondary structure elements. The conserved domains, including those designated Ras_like_GTPase (an N-terminal GTPase domain) and Dynamin_M (a middle domain), a GED, and a coiled-coil region, are marked.

Hoechst 33342 was used. The fixed cells were incubated with 20 μg/ml Hoechst 33342 for 10 min at room temperature. The cells were then washed three times with PBS. The preparations were further washed with PBS and mounted onto glass slides by using DABCO [1,4-diazbicyclo(2,2,2)octane; Sigma].

The fluorescent slides were then examined with an LSM 510 confocal laser scanning microscope (Zeiss, Germany) equipped with a 63× objective. Alexa green-labeled samples were excited at 488 nm by using an argon laser, and UV excitation was used to view Hoechst staining. Pictures were processed using an offline version of LSM 510 software (Zeiss).

Cellular proliferation. Different *E. histolytica* cells (with constructs expressing GFP, EhDLP1-GFP, and EhDLP1-K38A–GFP) were grown in the presence of 30 μg ml^{-1} G418, and the cells were counted by a hemocytometer at the times indicated in Fig. 8A. Cell viability was determined by microscopy using a trypan blue dye exclusion test.

RITC-dextran uptake. Pinocytosis was studied by observing the uptake of rhodamine isothiocyanate (RITC)-dextran as described before (13). The mid-log-phase cells were harvested, washed, and resuspended in fresh medium. The washed cells were then incubated with RITC-dextran (2 mg ml^{-1}; Sigma) for 30 min at 36°C, harvested, and washed with PBS. The cells were then resuspended in PBS containing 0.1% Triton X-100. The amount of endocytosed intracellular rhodamine was determined by measuring total fluorescence using a Cary fluorescence spectrophotometer.

Cytopathic assay. The ability of *E. histolytica* to kill target cells was studied using Chinese hamster ovary (CHO) cells as target cells. The destruction of a monolayer of CHO cells was assayed as described earlier (13). Briefly, trophozoites (2×10^5 ml^{-1} suspended in Dulbecco's modified Eagle medium [DMEM] without fetal calf serum) were added in triplicate to wells containing a confluent monolayer of CHO cells (2×10^5 ml^{-1}) prewashed with DMEM to remove traces of fetal calf serum, and the wells were incubated for 60 min at 37°C in an atmosphere of 95% air and 5% CO_2. The reaction was stopped by chilling the reaction mixture for 10 min, and the wells were then washed three times with cold PBS. The monolayer was fixed with 4% PFA for 10 min and stained with methylene blue (0.1% in 0.1 M borate buffer, pH 8.7). The excess stain was washed away with 0.01 M borate buffer, and the incorporated dye was extracted by adding 1.0 ml of 0.1 M HCl at 37°C for 30 min. The color was read in a spectrophotometer at 660 nm after appropriate dilutions with 0.1 M HCl. The destruction of cells was expressed in relation to the amount of dye extracted from the control monolayer of CHO cells.

Analysis of EhDLP1 expression in stressed cells by Northern blotting. Heat shock was administered by transferring proliferating *E. histolytica* cells into a water bath maintained at 42°C for 1 h. The cells were then chilled, and RNA was extracted. Cells were exposed to oxidative stress by being grown in 10 ml of complete TYI-S-33 medium in a 50-ml tissue culture flask for 1 h at 36°C with gentle shaking at 40 rpm. To achieve serum starvation conditions, the medium was replaced with TYI-33 medium containing 0.5% adult bovine serum for 24 h, and RNA was extracted.

Total RNA was purified using TRIzol reagent according to the instructions of the manufacturer (Invitrogen). RNA samples (30 μg) were resolved in formaldehyde agarose in a solution of gel running buffer (0.1 M MOPS [morpholinepropanesulfonic acid; pH 7.0], 40 mM sodium acetate, 5 mM EDTA [pH 8.0]) and 37% formaldehyde at 4 V/cm. The RNA was transferred onto GeneScreen Plus nylon membranes (NEN). Hybridization and washing conditions for RNA blots were per the manufacturer's protocol.

Sequence alignment and phylogenetic construction. Amino acid composition determination, restriction enzyme site analyses of DNA sequences, and multiple-sequence alignments (with CLUSTAL W) were performed using the BioEdit sequence alignment editor (version 7.0; Tom Hall). Secondary structure analysis of the protein sequence was carried out using PSIPRED (http://bioinf.cs.ucl.ac.uk/psipred/), NPS (9), and JPRED (8). Common predictions made by all three methods are reported.

Phylogenetic analysis of the extracted sequences from different organisms along with the *E. histolytica* sequence was done with the PHYLIP 3.67 package and the unweighted-pair group method using average linkages (UPGMA). The analysis was done with a bootstrap value of 100.

Miscellaneous methods. Standard molecular techniques, such as Western blot analysis, SDS-PAGE, Northern analysis, and protein estimation, were performed as described previously (24).

RESULTS

***E. histolytica* gene encoding DLP.** The *E. histolytica* genomic sequence was searched for the presence of a dynamin-1 gene by using standard bioinformatics methods. All analysis was done with the sequences available from TIGR (http://www.tigr.org) by using the first assembly as described by Loftus et al. (18). The primary annotation suggested the presence of a single dynamin-1-like gene (EH05370 in the TIGR database and EHI_013180 in Pathema) in the *E. histolytica* genome. However, the current annotation indicates the presence of three dynamin-like genes (Pathema database). Multiple-sequence alignment of all three genes was carried out to understand the relationship among these genes (see Fig. S1 in the supplemental material). A schematic representation of the alignment is shown in Fig. 1. The results indicated that all three predicted genes are homologs with high levels of sequence identity. One of these genes is unlikely to be functional due to its small size (Fig. 1). Therefore, the longest putative gene, EHI_013180 (EAL 44264), was used for further studies and is referred to hereinafter as the EhDLP1 gene.

The selected gene showed maximum similarity to the gene encoding dynamin-1-like protein isoform 2 of *Canis familiaris*. The identity of the gene products at the amino acid level was 60% and concentrated mainly at the amino termini of the proteins (see Fig. S2 in the supplemental material). The *E. histolytica* gene also displayed high levels of similarity to homologs from other eukaryotes, such as human, mouse, and *Dictyostelium*, suggesting that this gene is highly conserved across eukaryotes. EhDLP1 displays multiple domains (Fig. 1). These include a dynamin-specific N-terminal (GTPase) do-

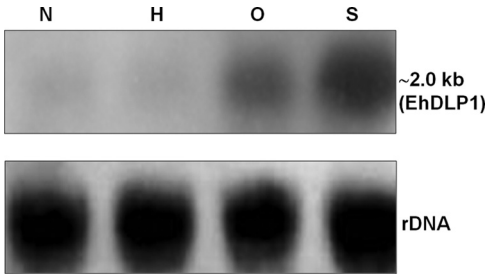

FIG. 2. Expression analysis of EhDLP1 in *E. histolytica* trophozoites. Total RNA was isolated from the trophozoites growing in log phase (N) or under different stress conditions: heat shock (H), oxygen shock (O), or serum starvation (S). RNA was run on a 1% agarose gel and transferred onto a nitrocellulose membrane. (Top) The blot was hybridized with radiolabeled EhDLP1 DNA as a probe, which gave an expected size at 2.0 kb. (Bottom) The same blot was rehybridized with rDNA to compare loading amounts.

main, a middle domain, and a GED. Typical nucleotide binding tripartite sequences (GSQSAGKSS, DLPG, and TKMD) corresponding to the amino acid positions 31, 134, and 203, respectively, were found. Secondary structure prediction for EhDLP1 was done using a number of programs available on the web. It revealed an overall helical structure with small stretches of β-strands and coiled-coil regions. Part of the GED exists as a long coiled-coil region at the C-terminal end of the protein (amino acids 510 to 570) (Fig. 1). A PXXP motif that may have a role in protein-protein interaction was also noticed at two places in the C terminus of EhDLP1 (amino acids 522 to 525 and 567 to 570). Such sequences have been described as sites for binding to Src homology 3 (SH3) domains present in many known partners of dynamins. No PH domain or PRD was identified in the sequence. The domain architecture of EhDLP1 suggests that it is a DLP and not a dynamin.

DLPs in other *Entamoeba* species. *E. dispar* and *E. invadens* genome databases (Pathema) were also searched for the presence of putative homologs of dynamin or DLP genes. The primary annotation suggested the presence of three such genes in *E. invadens* and two in *E. dispar*. The multiple-sequence alignment of all these genes along with the EhDLP1 gene revealed that all of them are likely to be orthologs. These results were further confirmed by domain analysis, which revealed the products to be potential DLPs (see Fig. S3 in the supplemental material).

Expression of EhDLP1 in *E. histolytica*. The expression of EhDLP1 in proliferating *E. histolytica* cells was checked by transcript analysis. Northern blots of total RNA isolated from mid-log-phase cells showed a faint band at about 2 kb, the expected size of the mature mRNA (Fig. 2). In order to check if EhDLP1 transcription is regulated by stress, EhDLP1 expression was evaluated under different stress conditions, such as heat shock, oxygen shock, and serum starvation (Fig. 2). Both oxygen shock and serum starvation significantly enhanced the accumulation of EhDLP1 transcripts. The level of transcripts in cells subjected to serum starvation was about sevenfold higher than that in control cells.

Subcellular localization of EhDLP1. The localization of EhDLP1 was checked by confocal microscopy using a polyclonal antibody raised against rEhDLP1. The recombinant

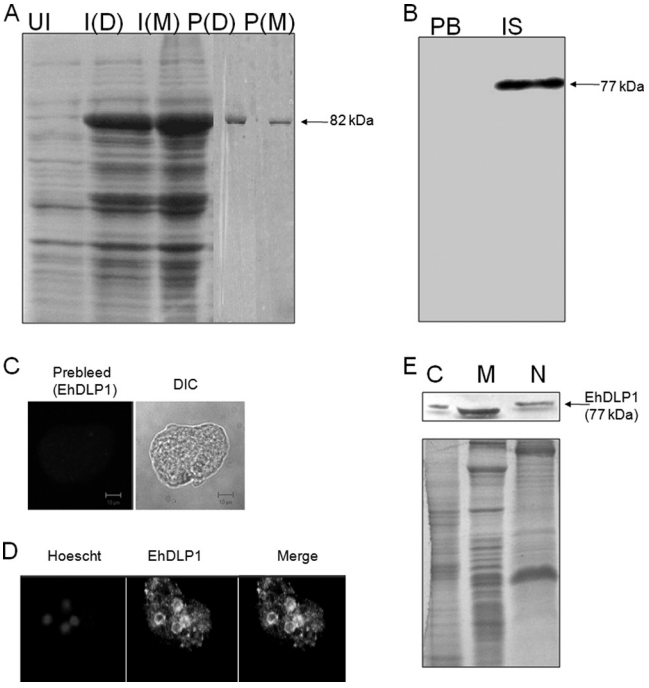

FIG. 3. Purification and subcellular localization of EhDLP1. (A) Genes for EhDLP1 and the lysine mutant were cloned into the pET-30(a) vector, and *E. coli* BL21(DE3) cells were transformed with the constructs. The cells were induced with IPTG, and the proteins were purified from the lysate by affinity chromatography using Ni^{2+}-NTA columns. The induced samples were resolved by SDS–10% PAGE. An induced band at about 82 kDa was seen. UI, uninduced sample; I(D), induced sample of EhDLP1; I(M), induced sample of mutant EhDLP1-K38A; P(D), purified EhDLP1; and P(M), purified mutant EhDLP1-K38A. (B) Fifty micrograms of *E. histolytica* whole-cell lysate was resolved by SDS–10% PAGE and transferred electrophoretically onto a polyvinylidene difluoride (PVDF) membrane. The blot was incubated with either preimmune sera (PB) or the polyclonal immune sera (IS) raised against rEhDLP1. The immune sera recognized a single band at the expected size of 77 kDa. (C and D) Log-phase trophozoites were fixed with 3.7% PFA and permeabilized with 1% Triton X-100. The cells were then stained with prebleed sera (C) or anti-EhDLP1 sera (1:50) (D). Hoechst was also used to stain the nuclei of the trophozoites. DIC, differential interference contrast. (E) Whole-cell lysate was prepared from the trophozoites growing in log phase and biochemically separated into cytoplasmic (C), membrane (M), and nuclear (N) fractions as described in Materials and Methods. Equal amounts (50 μg) of protein from all the fractions were resolved by SDS-PAGE, transferred onto PVDF membranes, and immunoblotted with anti-EhDLP1 as the primary antibody and anti-rabbit horseradish peroxidase as the secondary antibody. The lower panel shows Coomassie blue staining of the blot.

proteins (wild-type [WT] and mutant EhDLP1s) were purified as described in Materials and Methods (Fig. 3A). The antibody recognized a single band at 77 kDa from amebic lysate upon Western blot analysis, suggesting that it recognizes EhDLP1 specifically (Fig. 3B). While immunofluorescence visualization revealed no specific labeling with control antibody (Fig. 3C), the specific antibody displayed a very distinct pattern (Fig. 3D). Staining was found around the nucleus and throughout the cytoplasm. Most of the cytoplasmic staining was in the form of punctate spots. It is likely that EhDLP1 may be associated with some cytoplasmic membrane structures. Perinuclear localization was con-

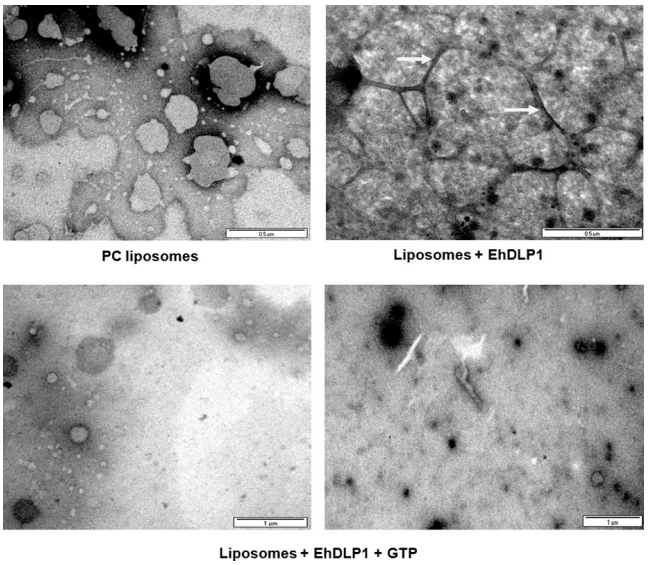

FIG. 4. EhDLP1 associates with and causes tubulation of lipid membranes. PC liposomes were prepared and incubated with buffer alone, rEhDLP1, or rEhDLP1 and GTP as described in Materials and Methods. Electron microscopy was performed for all three samples. EhDLP1 interacted with liposomes, which resulted in the formation of tubular structures (arrows) that disappeared upon incubation with GTP.

firmed by double labeling with DNA-specific dye Hoechst 33342. These observations were further confirmed by biochemical fractionation of amebic lysate and detection of EhDLP1 by Western blotting. The protein was detected in all the fractions, namely, the nuclear, cytoplasmic, and membrane fractions (Fig. 3E).

EhDLP1 produces membrane tubulation. Most DLPs are known to associate with membranes, and this association may lead to membrane tubulation. To test whether EhDLP1 could make membranes tubulate, a cell-free assay system was used. PC liposomes were prepared and incubated with EhDLP1. The structures formed were visualized using electron microscopy (Fig. 4). Lipid tubes were visible upon the incubation of EhDLP1 with the liposomes. These tubular structures underwent dissociation when GTP was added to the system. In the presence of GTP, small vesicles along with a few small tubulate structures were observed.

GTP binding and hydrolysis. Dynamins and DLPs show high rates of stimulated GTP hydrolysis, despite their low affinity for GTP. These proteins also have the property of self-assembling into large aggregates. Generally, these common characteristics are required for the functionality of dynamins or DLPs. In order to test if EhDLP1 also possesses these activities, GTP binding and hydrolysis assays were carried out. The lysine at position 38 was mutated to alanine in order to generate a GTPase domain mutant (EhDLP1-K38A).

GTP binding by EhDLP1 (WT) and the EhDLP1-K38A mutant was tested using UV cross-linking and filter binding assays as described in Materials and Methods. WT EhDLP1 bound radioactive GTP, as evident from the autoradiogram (Fig. 5A, lane 1). The binding was specific, as it was eliminated by competition with unlabeled GTP (Fig. 5A, lane 2). A faint

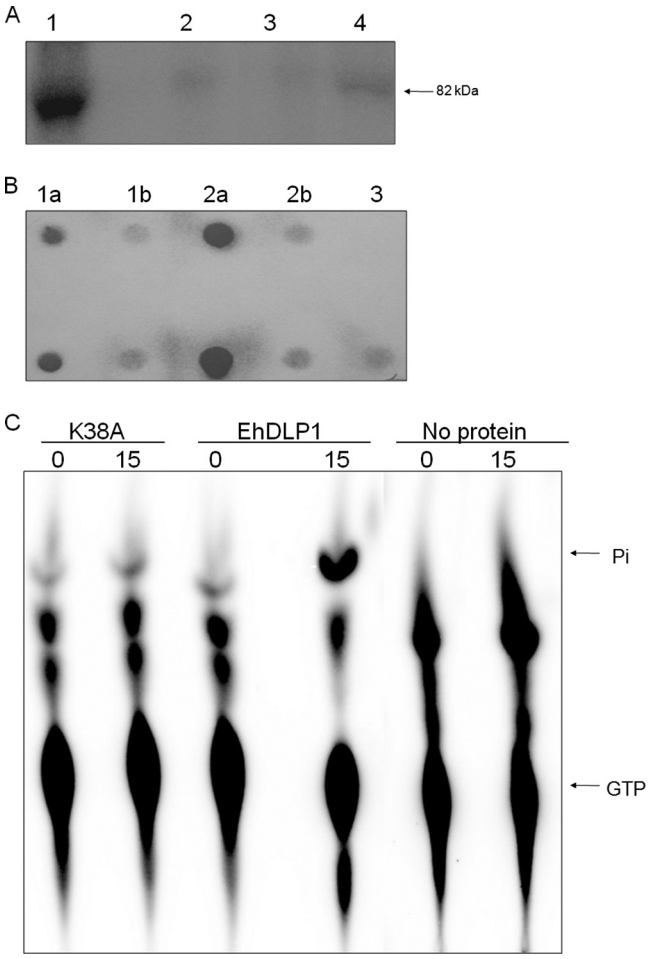

FIG. 5. GTP binding properties of rEhDLP1. (A) GTP binding by EhDLP1 (lanes 1 and 2) and EhDLP1-K38A (lanes 3 and 4) was checked by the UV cross-linking method. Cold GTP also competed for binding in lanes 2 and 4. SDS-PAGE separation and autoradiography were carried out to determine the extent of GTP binding. (B) GTP binding by both the WT and mutant EhDLP1 proteins was checked by a filter binding assay. In this assay, the protein was incubated with labeled GTP, or cold GTP competed for binding, and the reaction mixture was blotted onto a nitrocellulose membrane. The blot was washed quickly with the same buffer without labeled GTP, and autoradiography analysis was performed. Lanes: 1a and 1b, mutant protein; 2a and 2b, WT protein; 1a and 2a, labeled GTP; 1b and 2b, cold GTP competitor; 3, BSA control. (C) GTP hydrolysis was tested for both the WT and K38A mutant EhDLP1 proteins. Each protein was incubated with [γ-^{32}P]GTP in the GTPase buffer for 15 min at 37°C. The reaction was stopped, and the sample was spotted onto a polyethyleneimine TLC plate. The figure shows the autoradiogram of the TLC plate. Numbers at the top indicate minutes of incubation.

band was observed in the case of the mutant protein (EhDLP1-K38A) (Fig. 5A, lanes 3 and 4). The quantitative difference between the abilities of the two proteins to bind GTP was determined by a filter binding assay (Fig. 5B). The results showed that the K38A mutation reduced GTP binding by about 70%.

GTPase activities of the WT and mutant EhDLP1 were assayed by using [γ-^{32}P]GTP. The WT protein could hydrolyze GTP. The mutant protein had very little activity (Fig. 5C). These results indicate that EhDLP1 is a GTPase and that the

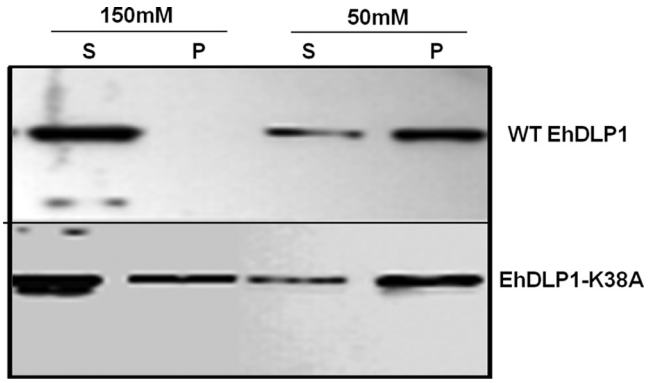

FIG. 6. EhDLP1 and EhDLP1-K38A form oligomers under low-salt conditions. (A) Samples of purified recombinant WT and mutant proteins (3 to 5 μg) were incubated in different salt concentrations (50 and 150 mM NaCl) and ultracentrifuged at 100,000 × g for 1 h to separate the supernatant (S) and pellet (P) fractions. Both fractions were separated by SDS–8% PAGE, electroblotted onto a nitrocellulose membrane, and visualized with anti-His antibody.

lysine at position 38 plays an important role in GTP binding and subsequent hydrolysis, as observed for other DLPs.

Ability to oligomerize under low-salt conditions. The ability of EhDLP1 to oligomerize in low-salt buffer was determined by a sedimentation assay. In the presence of 150 mM NaCl, EhDLP1 was found predominantly in the supernatant after ultracentrifugation, whereas only a small proportion was present in the pellet (Fig. 6). This finding suggests that EhDLP1 exists predominantly in a low-oligomeric state at high salt concentrations. On the other hand, more EhDLP1 was seen in the pellet than in the supernatant at a low salt concentration (50 mM), suggesting that the process of oligomerization is highly sensitive to the salt concentration. The same pattern was observed with the K38A mutant, suggesting that the ability to oligomerize in the presence of different salt concentrations is independent of GTP binding (Fig. 6).

Overexpression of GFP-tagged WT and mutant EhDLP1 proteins in *Entamoeba* trophozoites. In order to understand the function of EhDLP1 in the parasite, WT and mutant (K38A) EhDLP1 proteins tagged with GFP were expressed in *E. histolytica* cells. EhDLP1-GFP showed a distribution pattern similar to that of the endogenous EhDLP1, as GFP molecules were found around the cytoplasmic structures and nuclear membrane (Fig. 7). This result showed that the GFP tag did not alter EhDLP1 folding and thus its localization. Interestingly, the K38A mutant protein showed a very different staining pattern from the WT (Fig. 7). There was no specific labeling around any membrane-associated structures; the staining seemed to be diffuse throughout the cytoplasm. This shows that GTP binding and hydrolysis activities of EhDLP1 are required for sequestration of this protein to specific intracellular membranes.

Properties of *E. histolytica* cells overexpressing EhDLP1-K38A. In order to investigate the functional significance of EhDLP1, *E. histolytica* cells overexpressing the EhDLP1-K38A mutant were generated and the properties of these cells were studied. Cell lines carrying the pEh-NEO-GFP vector alone and cells expressing WT EhDLP1-GFP were used as controls.

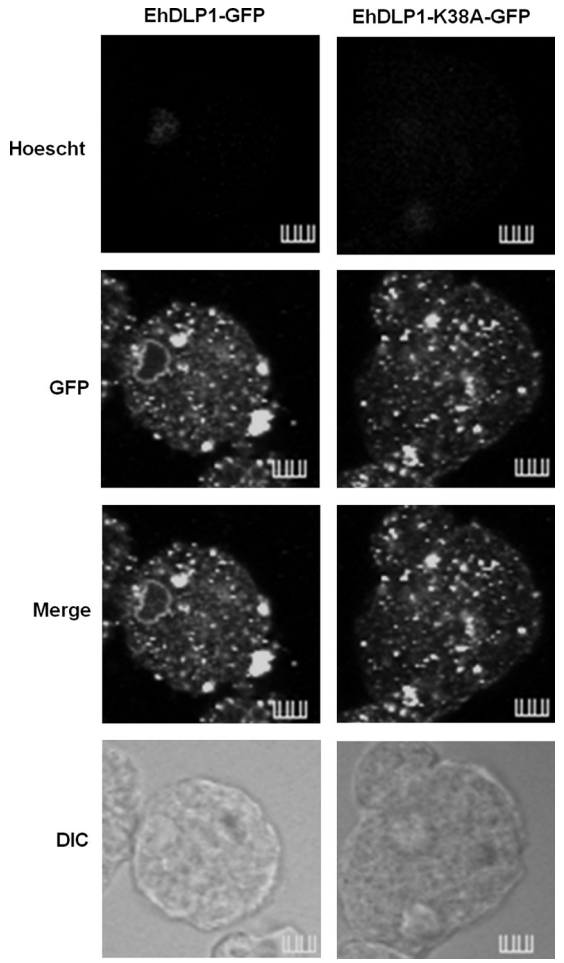

FIG. 7. Expression of WT and mutant EhDLP1 with GFP tags in *E. histolytica* trophozoites. *E. histolytica* trophozoites were transfected with a construct carrying GFP fused to EhDLP1 or EhDLP1-K38A. Immunolocalization of the tagged protein was achieved by staining with anti-GFP antibody. Hoechst 33342 was also used to stain the DNA in the nucleus. The bars represent 5 μm.

Effect on cellular proliferation. All three *E. histolytica* cell lines were checked for their proliferative abilities. Cells overexpressing EhDLP1-K38A–GFP displayed sluggish growth, and the cell number was reduced by 40% at 72 h (Fig. 8A). This was not due to cell death, as the slow-growing cells were found to be viable by a trypan blue test. The decrease in cellular proliferation upon the overexpression of EhDLP1-K38A clearly suggests that EhDLP1 plays an essential role in the growth of *E. histolytica* trophozoites.

Fluid phase endocytosis. Fluid phase endocytosis was measured by determining the level of uptake of a fluorescent marker, RITC-dextran. While EhDLP1-GFP cells showed a significantly higher level of fluid phase uptake than the cells carrying only GFP, no significant difference between cells overexpressing EhDLP1-K38A–GFP and EhDLP1-GFP was observed (Fig. 8B). This finding suggests that EhDLP1, particularly its abilities to bind and hydrolyze GTP, may have a role in fluid phase endocytosis.

Cytopathic activity. Cytopathic activity was measured using CHO cells. No significant differences in the abilities of the *E.*

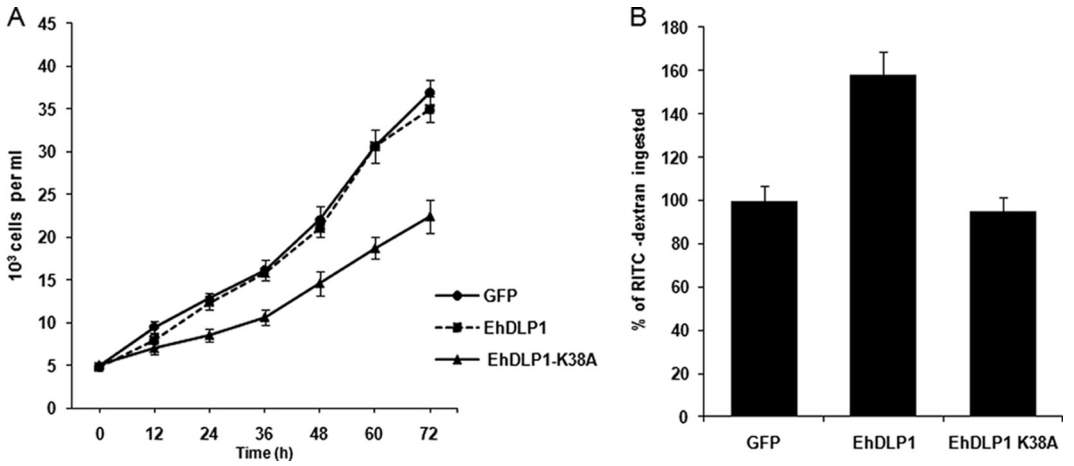

FIG. 8. Properties of cells overexpressing the WT and mutant EhDLP1 proteins. (A) The proliferation of *E. histolytica* cells expressing the indicated proteins is depicted. All transfectants were grown at 30 μg ml^{-1}, and the growth was measured by counting cells using a hemocytometer at the indicated time points after staining with trypan blue. (B) The ability to take up a fluid phase endocytic marker (RITC-dextran) was measured by incubating cells (grown at 30 μg ml^{-1} G418 for 48 h) with 2 mg ml^{-1} RITC-dextran in TYI-S-33 medium for 30 min. The intracellular fluorescence was evaluated as a measure of the uptake of RITC-dextran by using a spectrofluorimeter as described in Materials and Methods.

histolytic cells to kill the target cells were observed. The result suggests that EhDLP1 may not be involved in target identification or processes leading to cell death (data not shown).

Phylogenetic analysis. Since the GTPase domain showed the highest levels of matching with homologs, it was used to generate a phylogenetic tree. Sequences of DLPs and also dynamins from different organisms were obtained, and a phylogenetic tree was constructed using UPGMA from the PHYLIP package. The results suggested that the dynamin protein family forms several discrete clades (Fig. 9). Importantly, these clades contain functionally related dynamin family members. The major group contained proteins suspected to be involved in outer mitochondrial membrane fission in organisms from protists to fungi. EhDLP1 segregated with this group, suggesting a role of this protein in organelle division. *E. histolytica* does not possess a real mitochondrion, although a remnant of the mitochondrion, known as a mitosome, has been described previously (17, 27, 28). EhDLP1 may be involved in the division of mitosomes, although no evidence is available at the moment.

Other clades consisted of proteins responsible for vacuolar protein sorting, endocytosis via a clathrin pathway, outer chloroplast membrane fission, and inner mitochondrial membrane fission. Additional members of the dynamin family, including the Mx family of proteins involved in vertebrate response to viral infection, clustered separately. The tree was generated using the *E. coli* protein YjdA, which shares characteristics of dynamin family members, as an out-group.

DISCUSSION

The genome of *E. histolytica* contains three genes annotated to encode DLPs. The largest of these (the EhDLP1 gene) was studied using bioinformatics, biochemical, and cellular biological methods. Since orthologs of EhDLP1 were found in other *Entamoeba* species like *E. dispar* and *E. invadens* and the sequence was highly conserved across different phyla, it is likely to perform an essential function. A number of observations suggested that EhDLP1 is indeed a DLP. (i) Primary sequence analysis showed that EhDLP1 possesses all the domains common to DLPs. Although motif search programs did not show a PRD motif, a PXXP motif was noticed at two places in the C terminus of EhDLP1 (amino acids 522 to 525 and 567 to 570). These motifs may play an important role in the interaction of EhDLP1 with actin binding proteins. (ii) The protein has GTP binding, GTP hydrolysis, and oligomerization activities. (iii) It can associate with membranes and form tubular structures.

The phylogenetic analysis placed EhDLP1 in the largest group, which contained not only protist DLPs but also yeast and human DLPs. This group is functionally responsible for the fission of the outer mitochondrial membrane. *Entamoeba* is a lower eukaryote which lacks typical mitochondria, but it possesses mitosomes, a remnant of mitochondria without most of the proteins and DNA (27). So far, there has not been any study of organelle division and biogenesis in *Entamoeba*; therefore, it is difficult to speculate on the function of this protein. Its presence around the nucleus observed by immunofluorescence microscopy suggests that it may be involved in nuclear biology. The mechanism of nuclear division in *Entamoeba* differs from that in other eukaryotes, as the nuclear membrane does not disintegrate during nuclear division. Thus, it is likely that EhDLP1 is associated with the nuclear membrane and required for nuclear division. This association requires the ability of the protein to bind GTP, as evident from the mislocalization of the overexpressed GFP-tagged mutant protein. Mislocalization was also observed previously upon expression of GTPase mutants in *Caenorhabditis elegans* (16) and in mammalian cells (25). These results indicate that GTPase activity is crucial for association with organelle membranes and that EhDLP1 is functionally similar to other DLPs. Not many DLPs have been reported to be associated with the nuclear membrane. In animals, MxB regulates nuclear pore transport (14), and in *Tetrahymena*, Drp6 is required for macronuclear development (23). EhDLP1 is also visible as punctate spots in the cytoplasm. Though specific localization with the plasma membrane was not observed, some of the cytoplasmic staining may

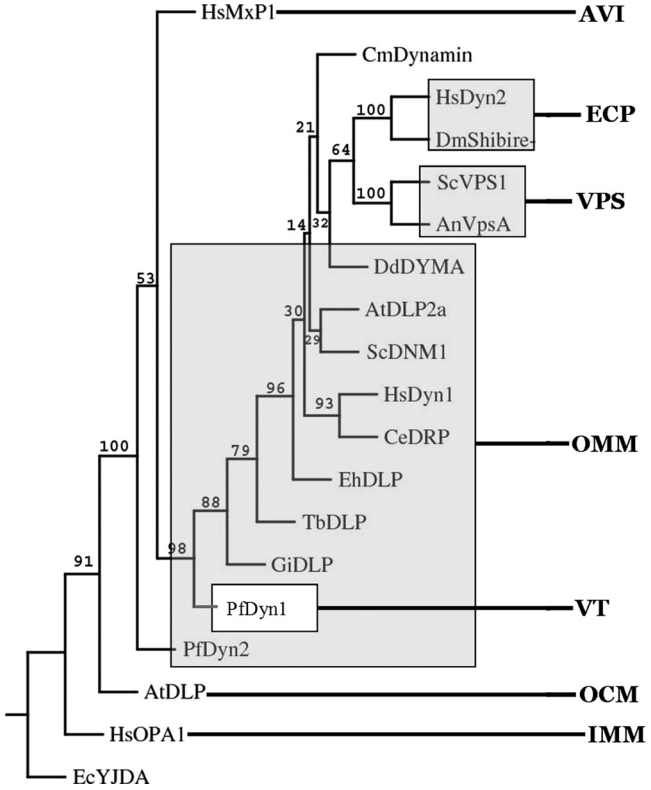

FIG. 9. Phylogenetic analysis of the GTPase domains of DLPs from various organisms. A phylogenetic tree was constructed using PHYLIP 3.67. GenBank or PlasmoDB accession numbers corresponding to the proteins used in this analysis are as follows: EhDLP1, EHI_013180; *Homo sapiens* OPA1 (HsOPA1), NP_056375; *Dictyostelium discoideum* DYMA (DdDYMA), CAA67983; *Arabidopsis thaliana* DLP2a (AtDLP2a), BAB85644; *Homo sapiens* Dyn1 (HsDyn1) and HsDyn2, NP_004399 and NP_004936; *Trypanosoma brucei* DLP (TbDLP), AAN05457; *Drosophila melanogaster* Shibire (DmShibire), P27619; *Plasmodium falciparum* Dyn1 (PfDyn1), PF11_0465 (in PlasmoDB); *Plasmodium falciparum* Dyn2 (PfDyn2), PF10_0368 (in PlasmoDB); *Saccharomyces cerevisiae* VPS1 (ScVPS1), AAA35216; *Aspergillus nidulans* VpsA (AnVpsA), BAB78398; *Giardia intestinalis* DLP (GiDLP), AAL87662; *Homo sapiens* MxP1 (HsMxP1), NP_002453; *Cyanidioschyzon merolae* dynamin (CmDynamin), AAO23012; *Saccharomyces cerevisiae* DNM1 (ScDNM1), P54861; *Caenorhabditis elegans* MGM1 (CeDRP), NP_495986; and *Arabidopsis thaliana* DLP (AtDLP), AAO89221. The *E. coli* YjdA protein (EcYJDA; AAA97008) was used as an out-group. The bootstrap values were based on 100 replicates. Proteins are grouped according to involvement in the following processes: AVI, antiviral infection; ECP, endocytosis via a clathrin pathway; VPS, vacuolar protein sorting; OMM, outer mitochondrial membrane fission; VT, vesicular trafficking; OCM, outer chloroplast membrane fission; and IMM, inner mitochondrial membrane fission.

be due to the association of EhDLP1 with vesicular membranes. The punctate spots may thus represent EhDLP1 association with some of the vesicular membranes. The trophozoites of *E. histolytica* possess several vesicles which may account for the number of spots observed in immunostaining. Such labeling and vesicular association have been reported previously for *Giardia* (11) and *Plasmodium* (7) species.

One of the consequences of the nuclear association of EhDLP1 may be its involvement in cellular proliferation. Overexpression of a mutated form of the molecule lacking GTPase activity did result in a dominant-negative phenotype of sluggish proliferation but not cell killing. DLPs from other organisms are known to be involved in endocytosis (6, 11, 20). It is likely that the amebic molecule may also be involved in this process, as our results obtained using a dominant-negative cell line did show a defect in endocytosis similar to that associated with other DLPs.

In conclusion, the results presented here show that *E. histolytica* DLP is similar to DLPs found in other organisms. It may have a role in organelle division and biogenesis. A detailed mechanistic study may help us to understand this important and hitherto unexplored aspect of *Entamoeba*.

ACKNOWLEDGMENTS

R.J. thanks UGC for the financial support throughout the study. S.S. acknowledges CSIR for financial assistance. We also acknowledge financial support from Jawaharlal Nehru University, Department of Science and Technology and Department of Biotechnology, Government of India.

REFERENCES

1. **Aley, S. B., Z. A. Cohn, and W. A. Scott.** 1984. Endocytosis in *Entamoeba histolytica*. Evidence for a unique non-acidified compartment. J. Exp. Med. **160:**724–737.
2. **Bernardo, S. M., Z. Khalique, J. Kot, J. K. Jones, and S. A. Lee.** 2008. *Candida albicans* VPS1 contributes to protease secretion, filamentation, and biofilm formation. Fungal Genet. Biol. **45:**861–877.
3. **Bredeston, L. M., C. E. Caffaro, J. Samuelson, and C. B. Hirschberg.** 2005. Golgi and endoplasmic reticulum functions take place in different subcellular compartments of *Entamoeba histolytica*. J. Biol. Chem. **280:**32168–32176.
4. **Breinich, M. S., D. J. Ferguson, B. J. Foth, G. G. van Dooren, M. Lebrun, D. V. Quon, B. Striepen, P. J. Bradley, F. Frischknecht, V. B. Carruthers, and M. A. Meissner.** 2009. A dynamin is required for the biogenesis of secretory organelles in *Toxoplasma gondii*. Curr. Biol. **19:**277–286.
5. **Cao, H., F. Garcia, and M. A. McNiven.** 1998. Differential distribution of dynamin isoforms in mammalian cells. Mol. Biol. Cell **9:**2595–2609.
6. **Chanez, A. L., A. B. Hehl, M. Engstler, and A. Schneider.** 2006. Ablation of the single dynamin of *T. brucei* blocks mitochondrial fission and endocytosis and leads to a precise cytokinesis arrest. J. Cell Sci. **119:**2968–2974.
7. **Charneau, S., I. M. Bastos, E. Mouray, B. M. Ribeiro, J. M. Santana, P. Grellier, and I. Florent.** 2007. Characterization of PfDYN2, a dynamin-like protein of *Plasmodium falciparum* expressed in schizonts. Microbes Infect. **9:**797–805.
8. **Cole, C., J. D. Barber, and G. J. Barton.** 2008. The Jpred 3 secondary structure prediction server. Nucleic Acids Res. **36:**W197–W201.
9. **Combet, C., C. Blanchet, C. Geourion, and G. Deleage.** 2000. NPS@: network protein sequence analysis. Trends Biochem. Sci. **25:**147–150.
10. **Dey, I., K. Keller, A. Belley, and K. Chadee.** 2003. Identification and characterization of a cyclooxygenase-like enzyme from *Entamoeba histolytica*. Proc. Natl. Acad. Sci. U. S. A. **100:**13561–13566.

10a. **Diamond, L. S., D. R. Harlow, and C. C. Cunnick.** 1978. A new medium for the axenic cultivation of *Entamoeba histolytica* and other *Entamoeba.* Trans. R. Soc. Trop. Med. Hyg. **72:**431–432.

11. **Gaechter, V., E. Schraner, P. Wild, and A. B. Hehl.** 2008. The single dynamin family protein in the primitive protozoan *Giardia lamblia* is essential for stage conversion and endocytic transport. Traffic **9:**57–71.
12. **Hinshaw, J. E.** 2000. Dynamin and its role in membrane fission. Annu. Rev. Cell Dev. Biol. **16:**483–519.
13. **Jain, R., J. Santi-Rocca, N. Padhan, S. Bhattacharya, N. Guillen, and A. Bhattacharya.** 2008. Calcium-binding protein 1 of *Entamoeba histolytica* transiently associates with phagocytic cups in a calcium-independent manner. Cell. Microbiol. **10:**1373–1389.
14. **King, M. C., G. Raposo, and M. A. Lemmon.** 2004. Inhibition of nuclear import and cell-cycle progression by mutated forms of the dynamin-like GTPase MxB. Proc. Natl. Acad. Sci. U. S. A. **101:**8957–8962.
15. **Konopka, C. A., J. B. Schleede, A. R. Skop, and S. Y. Bednarek.** 2006. Dynamin and cytokinesis. Traffic **7:**239–247.
16. **Labrousse, A. M., D.-L. Shurland, and A. M. van der Bliek.** 1998. Contribution of the GTPase domain to the subcellular localization of dynamin in the nematode *Caenorhabditis elegans*. Mol. Biol. Cell **9:**3227–3239.
17. **León-Avila, G., and J. Tovar.** 2004. Mitosomes of *Entamoeba histolytica* are abundant mitochondrion-related remnant organelles that lack a detectable organellar genome. Microbiology **150:**1245–1250.
18. **Loftus, B., I. Anderson, R. Davies, U. C. Alsmark, J. Samuelson, P. Amedeo, P. Roncaglia, M. Berriman, R. P. Hirt, B. J. Mann, T. Nozaki, B. Suh, M.**

Pop, M. Duchene, J. Ackers, E. Tannich, M. Leippe, M. Hofer, I. Bruchhaus, U. Willhoeft, A. Bhattacharya, T. Chillingworth, C. Churcher, Z. Hance, B. Harris, D. Harris, K. Jagels, S. Moule, K. Mungall, D. Ormond, R. Squares, S. Whitehead, M. A. Quail, E. Rabbinowitsch, H. Norbertczak, C. Price, Z. Wang, N. Guillén, C. Gilchrist, S. E. Stroup, S. Bhattacharya, A. Lohia, P. G. Foster, T. Sicheritz-Ponten, C. Weber, U. Singh, C. Mukherjee, N. M. El-Sayed, W. A. Petri, Jr., C. G. Clark, T. M. Embley, B. Barrell, C. M. Fraser, and N. Hall. 2005. The genome of the protest parasite *Entamoeba histolytica*. Nature **433:**865–868.

19. **Lohden-Bendinger, U., and T. Bakker-Grunwald.** 1990. Evidence for a vacuolar-type proton ATPase in *Entamoeba histolytica*. Z. Naturforsch. C **45:** 229–232.
20. **Morgan, G. W., D. Goulding, and M. C. Field.** 2004. The single dynamin-like protein of *Trypanosoma brucei* regulates mitochondrial division and is not required for endocytosis. J. Biol. Chem. **279:**10692–10701.
21. **Orozco, E., G. Guarneros, A. Martinez-Palomo, and T. Sanchez.** 1983. *Entamoeba histolytica*. Phagocytosis as a virulence factor. J. Exp. Med. **158:** 1511–1521.
22. **Praefcke, G. J., and H. T. McMahon.** 2004. The dynamin superfamily: universal membrane tubulation and fission molecules? Nat. Rev. Mol. Cell Biol. **5:**133–147.
23. **Rahaman, A., N. C. Elde, and A. P. Turkewitz.** 2008. A dynamin-related protein required for nuclear remodeling in *Tetrahymena*. Curr. Biol. **18:** 1227–1233.
24. **Sambrook, J., and D. W. Russell.** 2001. Molecular cloning: a laboratory manual, 3rd ed. Cold Spring Harbor Laboratory Press, Cold Spring Harbor, NY.
25. **Smirnova, E., D. L. Shurland, S. N. Ryazantsev, and A. M. van der Bliek.** 1998. A human dynamin-related protein controls the distribution of mitochondria. J. Cell Biol. **143:**351–358.
26. **Teixeira, J. E., and C. D. Huston.** 2008. Evidence of a continuous endoplasmic reticulum in the protozoan parasite *Entamoeba histolytica*. Eukaryot. Cell **7:**1222–1226.
27. **Tovar, J., A. Fischer, and C. G. Clark.** 1999. The mitosome, a novel organelle related to mitochondria in the amitochondrial parasite *Entamoeba histolytica*. Mol. Microbiol. **32:**1013–1021.
28. **Tovar, R., M. L. Murguia-Lopez, and M. De Lourdes Munoz.** 2000. Immunolocalization of clathrin during electron-dense granule secretion in *Entamoeba histolytica*. Arch. Med. Res. **31:**s143–144.
29. **van der Bliek, A. M., and E. M. Meyerowitz.** 1991. Dynamin-like protein encoded by the *Drosophila* shibire gene associated with vesicular traffic. Nature **351:**411–414.
30. **Weijak, J., L. Surmacz, and E. Wyroba.** 2003. Dynamin involvement in *Paramecium* phagocytosis. Eur. J. Protistol. **39:**416–422.
31. **Wienke, D. C., M. L. Knetsch, E. M. Neuhaus, M. C. Reedy, and D. J. Manstein.** 1999. Disruption of a dynamin homologue affects endocytosis, organelle morphology, and cytokinesis in *Dictyostelium discoideum*. Mol. Biol. Cell **10:**225–243.